Int J Adv Manuf Technol (2015) 81:387–396
DOI 10.1007/s00170-015-7163-6

ORIGINAL ARTICLE

Determining issues in optimal turning of micro-structured functional surfaces

Xu Zhang[1] · **Qiang Liu**[1] · **Xiaoqin Zhou**[1] · **Chao Lin**[2]

Received: 26 October 2014 / Accepted: 17 April 2015 / Published online: 8 May 2015

Abstract Micro-structured surfaces have received ever-increasing requirements in various fields, including optical systems, biological engineering, measurement system, and so on. Fast tool servo (FTS)-assisted ultra-precision diamond turning technique has been extensively regarded to be a very promising technology for the fabrication of the micro-structured functional surfaces with high efficiency and high surface quality. In this paper, the machining flowchart is thoroughly introduced; the key cutting parameters including tool geometry, diamond turning machine (DTM) slide carriage feedrate, and spindle speed are carefully investigated and determined to obtain optimal cutting performances during machining processes. Additionally, a novel toolpath generation method is proposed to minimize the volume of the toolpath data. Comparing with current method, the data volume generated by the new method can be significantly decreased by several times. Finally, the efficiency of the proposed cutting parameter determination method and the new toolpath generation method are verified by fabricating a typical sinusoidal grid surface.

Keywords Micro-structured surfaces · Fast tool servo · Cutting parameters · Toolpath generation · Diamond turning

✉ Qiang Liu
liu-qiang-1111@163.com

[1] School of Mechanical Science and Engineering, Jilin University, Changchun, China

[2] Space Optics Research Laboratory, Changchun Institute of Optics, Fine Mechanics and Physics, Chinese Academic of Sciences, Changchun, China

1 Introduction

Micro-structured functional surfaces have received ever-increasing requirements in optical systems, biological engineering, and measurement systems and so on [1–4]. However, it is still a challenge to fabricate these surfaces with high quality and high efficiency due to their complicated shapes. Fast tool servo (FTS)-assisted ultra-precision diamond turning technique has been extensively regarded to be a very promising technology for the fabrication of the micro-structured functional surfaces [5–11].

As for the typical FTS machining system, workpiece is clamped on the spindle, FTS is fixed on slide carriage of diamond turning machine (DTM) which can move along z-axis direction and *x*-axis direction. During the fabrication process, FTS drives the cutting tool moving back and forth at a high frequency to obtain various complex surfaces. Generally, FTS working frequency is several times of spindle rotational frequency which is determined by the shapes of the optics. High-precision toolpath and the optimal cutting parameters are two critical elements for fabricating high-quality micro-structured surfaces. Unfortunately, most of previous studies have mainly focused on the design of FTS system to obtain higher performances, such as long stroke, high working bandwidth, and high positioning accuracy. The optimal determination of the cutting parameters has been ignored. Lu et al. introduced that the quality of the FTS diamond turned micro-structured surfaces depended mainly on the cutting speed and FTS working frequency [8], and studied the generation characteristics of micro-structures for surface texturing applications when clearance angle of the cutting tool is smaller than this critical angle [9]. Neo et al. processed a novel method to extend the FTS-limited stroke length with layered tool trajectories [10]. Although certain issues of the determination process have been mentioned, thorough studies of the process are

lacking [11]. Motivated by this, the main objective of this paper is to give a complete investigation and guidance for the selection of optimal cutting parameters and the optimal toolpaths with respect to various cutting conditions.

Generally, the cutting parameters include diamond tool geometry, spindle speed, and DTM feedrate. The tool geometry and feedrate must be optimized before toolpath generation processes. If the tool geometry is not carefully optimized, over-cutting and tool interference may happen during the fabrication process resulting in deteriorated quality or even destroy of machined surfaces. As is well known, the feedrate of cutting tool along the *x*-axis of DTM will directly determine the heights of surface residual tool marks, which dominates the machining errors in mid-spatial frequencies. The spindle speed is the critical element to guarantee succeeding machining process which is decided by FTS dynamics performance and workpiece surface geometry.

Currently, the toolpath calculation process is based on uniformly discrete angles of the local cylindrical-coordinate system. Reference points are first chosen in the xoy plane with equal central angle interval, and then projected onto the given micro-structured surfaces to obtain the tool contact points (TCPs), accordingly determining the tool location points (TLPs) [12–14].

During the practical cutting process, the linear interpolation is usually employed to fit the toolpath by FTS controller. The defects of the existing toolpath can be summarized as follows: The TCPs are not uniformly distributed which become sparser with workpiece radius increasing and resulting in greater form errors of machined surfaces with complex surface shapes [14, 15]. To the best knowledge of the authors, no pertinent literatures can be found to give guidance of the reference point selection in the xoy plane. So, what will be the appropriate interval angle between adjacent reference points? The smaller the interval angle is, the more accurate surface will be obtained just at the expense of massive data of the TCPs. For instance, to guarantee the machining accuracy, the toolpath data file obtained by Gao W et al. is so vast (approximate 3 GB) when fabricating a sinusoidal grid surface with 150 mm diameter [13].

In this paper, the flowchart of fabricating micro-structured functional surfaces by FTS-assisted diamond turning is detailed, and the two critical issues, namely, the optimal selection of cutting parameters and the optimal toolpath determination process, are deliberately discussed. To ensure the machining accuracy with minimum volume of toolpath data, the new toolpath generates the TCPs directly from the perspective of the interpolation principle. Finally, following the proposed parameter determination methods, a sinusoidal grid surface is fabricated to validate the efficiency of the proposed method.

2 Working principle of FTS-assisted diamond turning

The flowchart of FTS-assisted diamond turning process is illustrated in Fig. 1. The tool shape must be carefully determined firstly to avoid over-cutting and cutting interference for any given micro-structured surfaces, and the feedrate which will directly affect surface roughness should be further determined. After the critical tool shape and the feedrate chosen, the toolpath can accordingly be calculated and decomposed into two parts that implemented by the spindle and FTS, respectively. Then, the spindle speed is obtained considering the constraints of FTS working performance and the motion trajectories decomposed from the toolpath. By finely harmonizing the cutting parameters of the system, optical surfaces with high accuracy and high surface quality can be sufficiently achieved. More details about the optimal selection process are detailed in section 3.

3 Determination of optimal cutting parameters

3.1 Determination of optimal tool shape

Diamond tool shape parameters mainly consist of tool nose radius, included angle, clearance angle, and rake angle. The cutting tool with zero rake angle is commonly utilized in practical turning process. As for the tool with non-zero rake angle, the pose changes induced by the angle should be deliberately compensated [5]. The selection process of the tool nose radius is crucial for two reasons: (1) it directly influences the

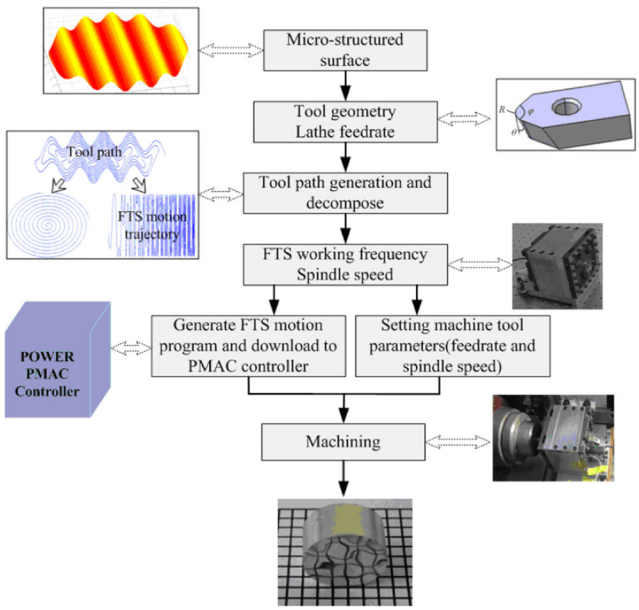

Fig. 1 Flowchart of FTS diamond turning micro-structure surfaces

roughness of machined surfaces and (2) the tool with unsuitable nose radius will induce undesired over-cutting phenomenon, accordingly decrease the accuracy of machined components [14]. The included angle and clearance angle should also be carefully selected to avoid cutting interferences. Fang et al. introduced the selection process of the tool nose radius and the included angles; however, systematic research works are still lacking [5]. Otherwise, with the increasing complexity of microstructured surfaces, cutting interference between the tool flank face and the machined surface will be much easily to be occurred. Thus, the tool clearance angle must be examined carefully.

1. Determination of the radius and the included angle of the tool

   In view of the workpiece rotation during turning process, the whole surface is decomposed into a series of two-dimensional sectional curves along the radius direction which are all through the origin of the spindle coordinate as shown in Fig. 2. To avoid over-cutting phenomenon, the curvature radius at any point on the surface should be larger than the radius of the cutting tool. Besides, the included angle φ_t should be smaller than $2\varphi_{i,j}$, where $\varphi_{i,j}$ is the desired surface related angle as shown in Fig. 2b. In the cylindrical coordinate of DTM, the desired freeform surface can be expressed as follows:

$$z = f(\rho, \theta) \tag{1}$$

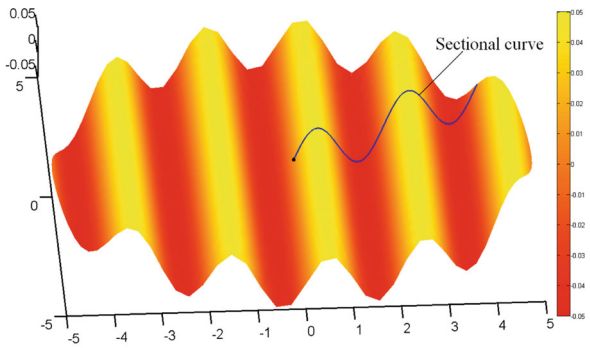

(a) Sectional curve method

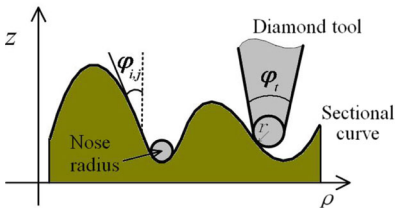

(b) Calculation of nose radius and included angle

Fig. 2 Sectional curve method for calculating tool geometry. **a** Sectional curve method. **b** Calculation of nose radius and included angle

The curvature radius $\rho_{i,j}$ at any given point $P_{i,j}(\rho_i,\theta_j)$ on the decomposed curve can be expressed as follows:

$$\rho_{i,j} = \left| \frac{\left(1 + \frac{\partial z}{\partial \rho}\right)^{\frac{3}{2}}}{\frac{\partial^2 z}{\partial \rho^2}} \right| \quad \rho = \rho_i, \theta = \theta_i \tag{2}$$

The corresponding angle $\varphi_{i,j}$ can be obtained as follows:

$$\varphi_{i,j} = \arctan\left(\frac{1}{\partial z / \partial \rho}\right)\Bigg|_{\rho = \rho_i, \theta = \theta_i} \tag{3}$$

By calculating the minimum value of $\varphi_{i,j}$ and minimum value of the concave curves curvature radius R_s on the sectional curves, tool nose radius R_t and included angle φ_t are optimized, respectively, which can be expressed as follows:

$$\begin{cases} R_t \geq \max\left(\rho_{i,j}, \forall i, \forall j\right) \\ \varphi_t \leq 2\min\left(\varphi_{i,j}, \forall i, \forall j\right) \end{cases} \tag{4}$$

2. Determination of the tool clearance angle

   As shown in Fig. 3, the initial toolpath is calculated firstly and unwrapped with respect to helix in the xoy plane. The unwrapped curve is expressed as $f(l)$ where l is actual arc length of the plane helix. Enlarged view of region A of the unwrapped toolpath for a typical sinusoidal surface as shown in Fig. 3b is illustrated in Fig. 4, where R' is the tool clearance angle and θ_1 is the acute angle between the tangent line of $f(l)$ and the abscissa axis when $f'(l)<0$.

   It is evident that the cutting interference phenomenon between the tool flank face and the desired surface occurs only when $f'(l)<0$. In order to avoid the unwanted interference, the tool clearance angle θ_t' must be greater than the maximum value of θ_1. The relationship between $\max(\theta_1)$ and $f'(l)$ can also be expressed as follows:

$$\tan\theta_{1\max} = -\min\left(f'(l)\right) \tag{5}$$

Therefore, the tool clearance angle must meet the condition as follows:

$$\theta_t' > \arctan\left(-\min\left(f'(l)\right)\right) \tag{6}$$

3.2 Determination of optimal feedrates of the machine tool

After determining the cutting tool shapes, surface roughness which is dominated by surface scallop-height is mainly influenced by the feedrate of DTM. Generally, the surface scallop-

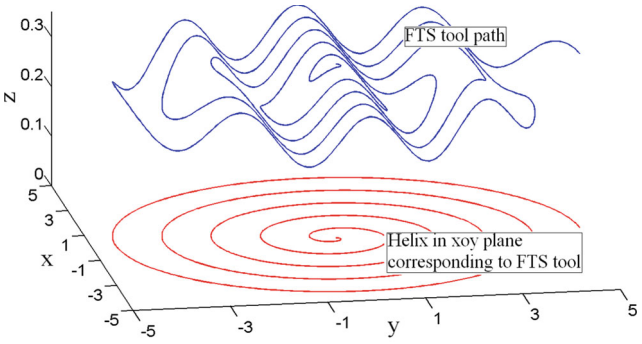

(a) Initial tool path

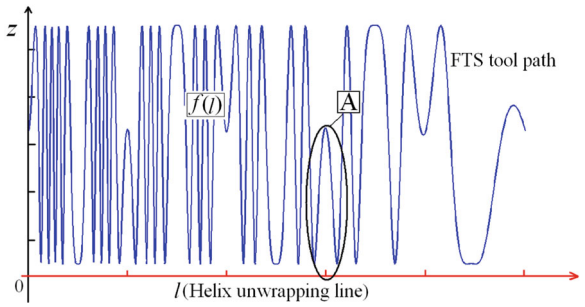

(b) Tool path unwrapped line

Fig. 3 Toolpath and unwrapped line. **a** Initial tool path. **b** Tool path unwrapped line.

heights highly depend on the curvature of the surfaces as shown in Fig. 5, and they can be calculated as follows [16]:

$$\text{Convex surface: } H_1 = \sqrt{(R'+R_t)^2-(f/2)^2}-\sqrt{R_t^2-(f/2)^2}-R'$$

$$\text{Concave surface: } H_2 = R'-\sqrt{(R'-R_t)^2-(f/2)^2}-\sqrt{R_t^2-(f/2)^2}$$

$$\text{Flat surface: } H_3 = R_t-\sqrt{R_t^2-(f/2)^2}$$

where R' is the curve curvature radius. Obviously, $H_2>H_3>H_1$

Therefore, the maximum surface scallop-height will be occurred at the concave surfaces with minimum curvature radius in the sectional curves. With the known value of minimum curvature radius R_s and tool nose radius R_t, feedrate f can be calculated with required surface scallop-height H by solving the formula:

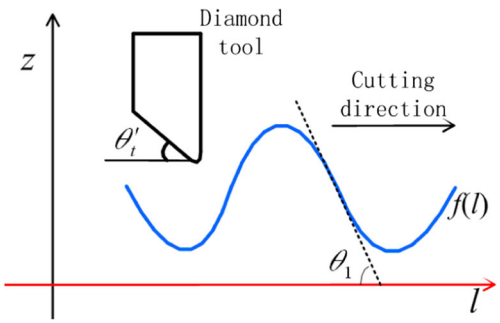

Fig. 4 Schematic diagram of cutting the sinusoidal surface

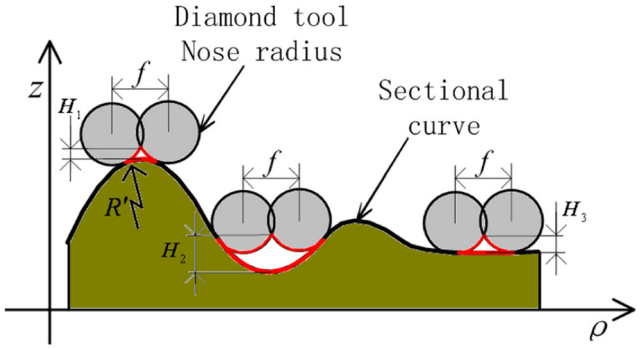

Fig. 5 Schematic diagram of surface scallop-height

$$H = R_s-\sqrt{(R_s-R_t)^2-(f/2)^2}-\sqrt{R_t^2-(f/2)^2} \tag{7}$$

3.3 Determination of the spindle speed

FTS working frequency and spindle speed which is usually selected by experience are much lower than there ultimate working performance to ensure the cooperation of the FTS system and DTM. Actually, DTM spindle speed is limited by FTS working performance, as well as the geometry of machined surface. The relationship of DTM spindle speed and FTS working frequency must be analyzed to guide how to select the spindle speed.

After toolpath of given surface calculated with known tool radius and feedrate by some kinds of toolpath generation methods, it is decomposed into two parts: the spiral trajectory in xoy plane implemented by DTM and the oscillations along the z-axis direction conducted by FTS which will be used to determinate spindle speed. FTS motion trajectory of the surface shown in Fig. 2 can be described in Fig. 6 where the abscissa axis is the spindle revolution. It can be seen that the working frequency of the FTS is multiple of the spindle speed. The Fourier transform is applied to the trajectory to obtain its features in frequency domain shown in Fig. 7. The maximum frequency component is about 15 times of that of the spindle while some high-frequency components with very small amplitudes are neglected. It means that FTS maximum working frequency is 15 Hz if spindle speed is 1 r/s. The amplitude and working frequency of FTS system are different with different freeform surfaces and different places of the same surface. FTS motion trajectory must be strictly corresponding to spindle speed. While the spindle is capable of very high rotational speed, FTS working bandwidth will be the key factors to constrain the machining efficiency.

In view of the working bandwidth f_F obtained by sine sweep tests, the maximum rotational speed $v_{\max}$ (r/s) of the spindle can be expressed as follows:

$$v_{\max} = f_F/m \tag{8}$$

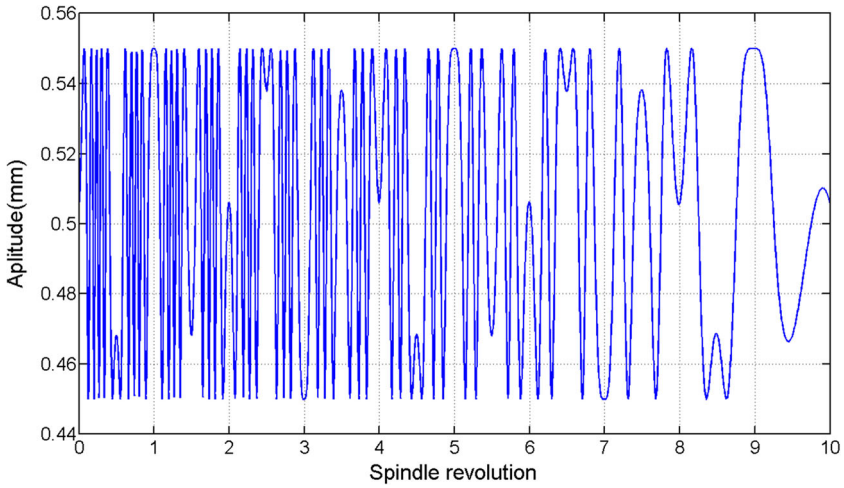

Fig. 6 The toolpath in terms of the spindle revolution

where m is the maximum multiple between FTS working frequency and spindle speed obtained from Fig. 7.

4 Iso-error toolpath calculation method

As for current toolpath generation methods, the most crucial problem is how to select cutting points to fit the ideal toolpath with enough accuracy and minimum toolpath data file. An effective way to deal with this problem is the real-time linear interpolation according to the continuously changing surface curvature as shown in Fig. 8.

4.1 The principle of new toolpath calculation

In view of the cylindrical coordinate of the machine tool, the following formula can be obtained to describe the motions of the machine tool:

$$\rho = R - f \cdot \varphi / (2 \cdot \pi) \tag{9}$$

where R is the workpiece radius, φ is the spindle rotation angle, ρ is the radius of the cutting point, and f is the machine tool feedrate. As for a given point $P_i(\rho_i, \varphi_i, z_i)$, its position can be expressed as follows:

$$\begin{cases} \varphi_i = \varphi_i \\ \rho_i = R - f \cdot \varphi_i / (2\pi) \\ z_i = f(\rho_i, \varphi_i) \end{cases} \tag{10}$$

1. Linear interpolation principle

   Considering the interpolation motions between any two adjacent cutting points, the desired interpolation error e and the interpolation chord L as shown in Fig. 9 yield the following:

$$\begin{cases} e = R' \left(1 - \cos\left(\frac{\delta}{2}\right)\right) \\ L = 2 \cdot R \cdot \sin\left(\frac{\delta}{2}\right) \end{cases} \tag{11}$$

   where R' is the curvature radius and δ is the central angle corresponding to L.

   As shown in Fig. 8, o is the center of plane spiral curve and $\Delta\varphi_i$ is the interval angle between two adjacent subpoints projected by cutting points P_i and P_{i+1}; the

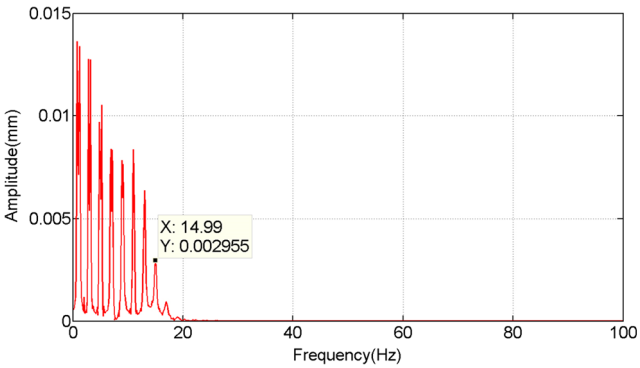

Fig. 7 Frequency spectrum of toolpath in terms of the spindle revolution

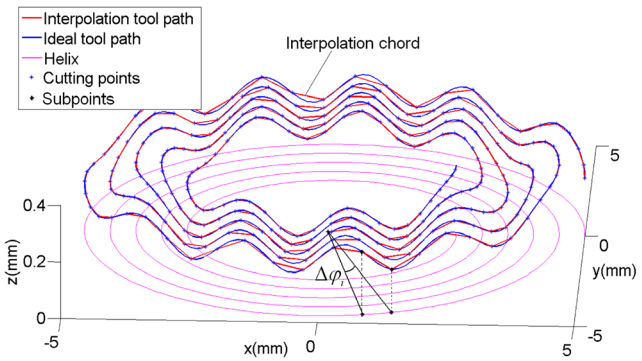

Fig. 8 Real-time linear interpolation toolpath generation method

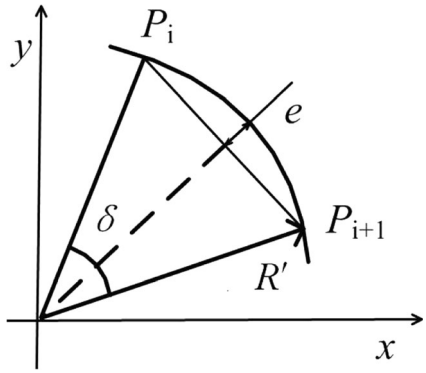

Fig. 9 Linear interpolation principle

relationships between L, P_i, and $\Delta\varphi_i$ can be obtained as follows:

$$(z_i - z_{i+1})^2 + (\rho_i \times \Delta\varphi_i)^2 = L^2 \tag{12}$$

Due to the complexity of the micro-structure surfaces, the surface curvature radius R' as well as $\Delta\varphi_i$ may change continuously, and a number of calculate results may be obtained while solving formula (12) directly. This phenomenon will bring troubles to the calculation process. Therefore, in this method, the cutting points are calculated by increasing the chord with a certain length step by step until the actual interpolation error is greater than desired error e. The chord increased at the first time is $L_{\min}/4$. $L_{\min}$ is the interpolation chord at minimum curvature radius curve which can be calculated when calculating the tool clearance angle. Formula (12) will be changed into

$$(z_i - z_{i+1})^2 + (\rho_i \times \Delta\varphi_i)^2 = {L_{i,j}}^2 \tag{13}$$

where $L_{i,j}$ is the chord length between i-th and $(i+1)$-th cutting point after stepping increased j times and $L_{i,j}=j\cdot L_{\min}$.

2. Calculation of interpolation error

The schematic of the interpolation error is shown in Fig. 10. It can be seen that the actual maximum interpolation error e_r is difficult to be obtained due to the continuously changing surface curvatures. e_r' is the interpolation error at midpoint of chord L which is usually greater than e_r. Therefore, e_r is replaced by e_r' in the actual interpolation process in this method. The error e_r' can be calculated by:

$$e_r' = |[z_A + z_B]/2 - z_C| \tag{14}$$

That is,

$$e_r' = |[f(\rho_A, \varphi_A) + f(\rho_B, \varphi_A + \Delta\varphi_i)]/2 - f(\rho_C, \varphi_A + \Delta\varphi_i/2)| \tag{15}$$

While $\Delta\varphi_i$ can be obtained by calculating formula (10), formula (11), and formula (13), e_r' is obtained by solving formula (15). If the calculated value e_r' is smaller than the given value e_r, the chord length L_{ij} increases to calculate larger $\Delta\varphi_i$ and e_r until $e_r' \geq e$ which the corresponding interval angle $\Delta\varphi_i$ can be obtained, as well as the coordinate position of P_{i+1}.

3. Some key points

Generally, a micro-structured surface contains some key points, such as inflection points and discontinuity points. These places are much easier to generate machining errors during the cutting process as shown in Fig. 11. These points must be calculated carefully. Generally, the sign of the first derivative or second derivative will be changed when encountering an inflection point or a discontinuity point. The step increase of chord must be stopped while encountering these points and calculate the corresponding interval angle $\Delta\varphi_i$ and cutting points P_{i+1}.

Using FTS controller's function of external time-base control, spindle rotation angle is measured by an encoder to instead of time as the fictitious "time" which means that the FTS motions are position-vs-angle trajectories instead of position-vs-time trajectories. The working frequency of the FTS will vary along with the changes of spindle speeds. This function will improve the corporation ability of FTS system and DTM and reduce the influence of spindle speed drifting. Therefore, the interval angle between arbitrary adjacent cutting points must be calculated and saved with respect to FTS trajectories.

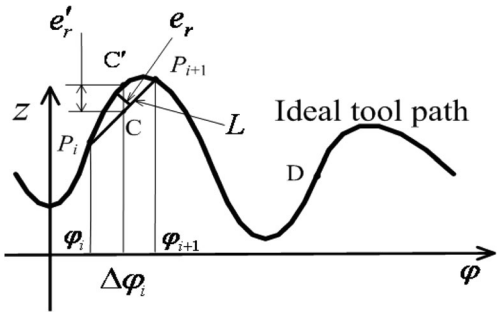

Fig. 10 Interpolation error schematic diagram

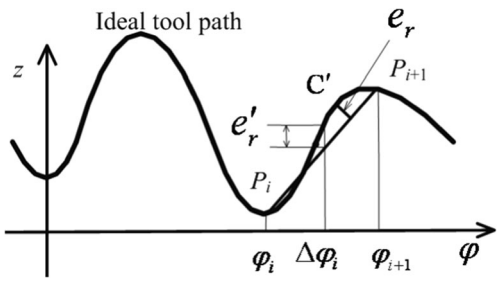

Fig. 11 Key points which are easy to generate machining errors

4.2 Toolpath calculation flowchart and calculation example

For sake of clarity, the toolpath calculation flowchart is emphasized in Fig. 12.

Figure 13 shows the toolpath for a typical sinusoidal grid micro-structured surface which are calculated by conventional equal-angle method and the new real-time interpolation method, respectively. The radius, the wavelength, and the amplitude of the surface are 0.2, 0.1, and 0.02 mm, respectively. The feedrate is 0.01 μm and tool radius is 0.5 mm. From Fig. 13a, it can be seen that the subpoints in xoy plane which are projected by the cutting points are irregularly distributed. The minimum interval central angle of new path is 0.0298 and the number of cutting points is 1638. While for the equal-angle method shown in Fig. 13b, in order to ensure the accuracy of the surface, the interval angle is also 0.0298, while the cutting points number is 4217. Evidently, the real-time linear interpolation method can significantly reduce the volume of toolpath data file by 2.57 times which expresses the superiority of the new toolpath. The superiority will be different with different micro-structured surfaces.

5 Cutting experiments

Cutting experiment is carried out following the flowchart and using the new toolpath. The experiment is implemented on a DTM with a voice coil motor (VCM)-actuated FTS as shown in Fig. 14. The workpiece is clamped on the spindle and the FTS is mounted on the slide which can move along the x direction and the z-axis direction of the DTM.

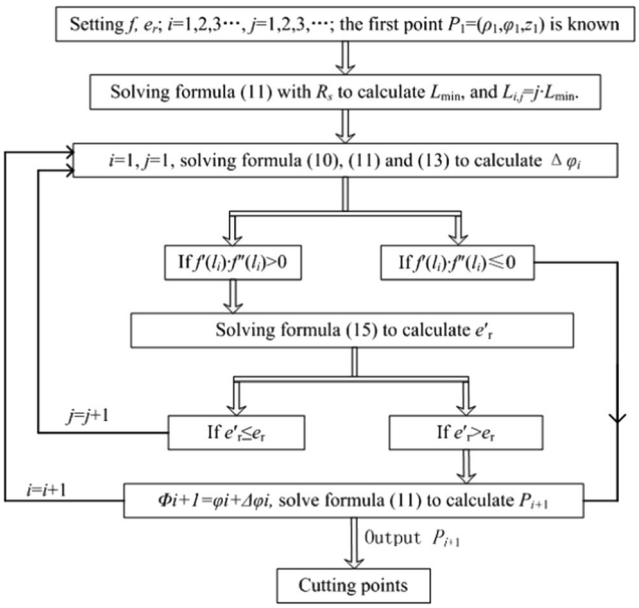

Fig. 12 Toolpath calculation flowchart

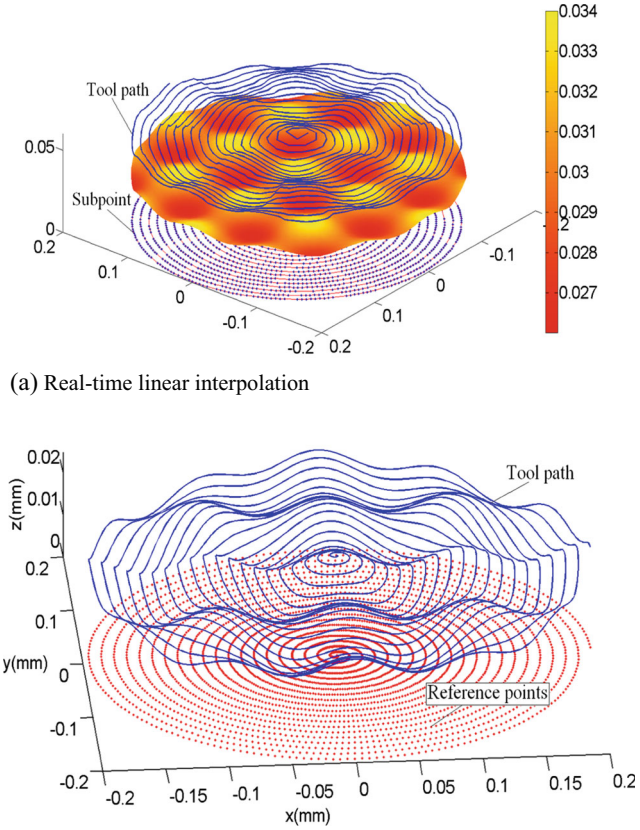

(a) Real-time linear interpolation

(b) Equal-angle method

Fig. 13 Toolpath generated by equal-angle method and real-time linear interpolation method. **a** Real-time linear interpolation. **b** Equal-angle method

A sinusoidal grid surface with wavelength of 2.5 mm is machined on a 6061 aluminum bar. A PCD cutting tool is employed in this experiment, and the tool geometry parameters are calculated and presented in Table 1.

Initial toolpath of the sinusoidal grid surface is calculated shown in Fig. 15. The FTS motion trajectory and the corresponding frequency spectrum are described in Fig. 16a, b, respectively. It can be seen that maximum frequency component about 12 times of that of the spindle. With respect to the closed-loop bandwidth of the FTS f_F is 60 Hz, the maximum speed of the spindle can be obtained by Eq. 8 which is 5 r/s. The feedrate is calculated according to Eq. 7 with the constraint scallop-height of 20 nm, and the obtained optimal feedrate is about 5.3 μm. Therefore, in this cutting experiment, the spindle speed is selected to be 1 r/s; the feedrate is 5 μm/r. The actual toolpath of the sinusoidal grid surface is shown in Fig. 17a, and the FTS performance is tested by following this signal that the following error is about 0.5 % (Fig. 17b, c). The FTS motion revolution is 0.08 μm shown in Fig. 17d.

The photo of machined surface is shown in Fig. 18a. OLS3000 Laser Scanning Confocal Microscope is used to capture the micro-topographies of the machined surface. The measured result is shown in Fig. 18b. The obtained surface

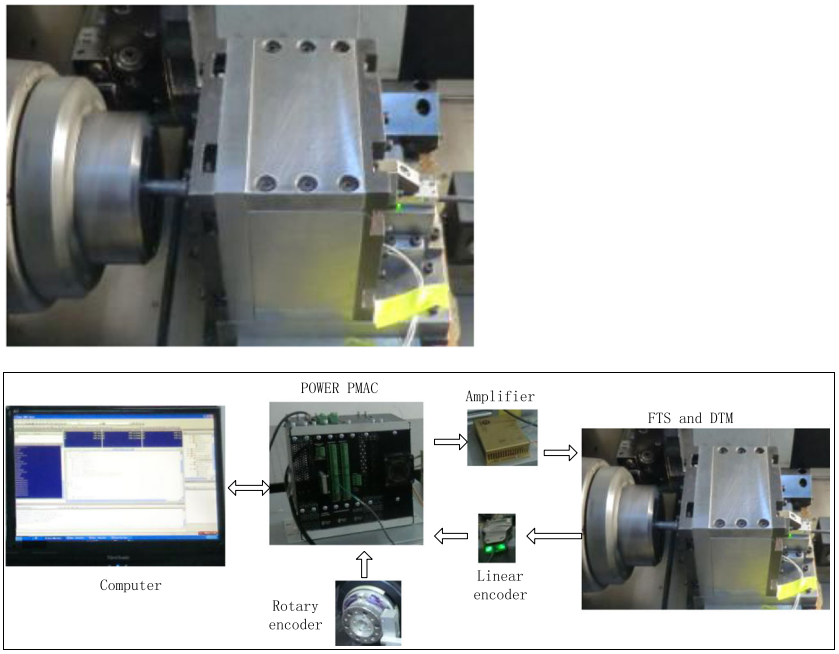

Fig. 14 DTM and VCM actuated FTS system

roughness is about Ra 32 nm which is much higher than the preset values. In the actual cutting process, except the main factors of tool geometry and feedrate, surface roughness is also influenced by workpiece material, cutting vibration, and tool wear. In Fig. 18b, it can be seen that there are some black spots on the workpiece surface which mainly are the material defects, such as the impurities or sand holes. The surface roughness is increased by these defects distributing in the surface. The defects also increase the cutting vibration to increase the surface roughness. The surface profile of micro-structured surface or other complex surfaces are usually measured by high-cost equipments or other self-designed measurement devices, and a precision and simple measurement device is being developed. Therefore, the machined surface profile error is not discussed in this paper.

6 Conclusion

In this paper, the flowchart of micro-structured surfaces fabricated by FTS diamond turning is thoroughly described. The machining parameters are first completely and thoroughly introduced. Especially, the tool clearance angle is calculated to avoid cutting interference. The DTM feedrate is calculated according to surface roughness while the accurate feedrate greatly improves machine efficiency with satisfactory surface quality. The relationship between spindle speed and FTS working performance is established which optimum FTS working performance and maximum spindle speed can be obtained for high precision and high machining efficiency.

The novel toolpath generation method based on real-time linear interpolation is proposed for the FTS-assisted diamond turning of micro-structured surfaces. The new toolpath can greatly reduce the volume of toolpath file with desired surface profile accuracy. The more complex the surface geometry, the effect of the new toolpath is better. A testpiece of a typical sinusoidal grid surface is fabricated following the flowchart and using the new toolpath. Considering the difficulty and high cost of measuring the machined micro-structured surfaces, the measurement of the surface profile is not discussed in this paper.

On the whole, the purpose of this research is to thoroughly introduce the machining flowchart of micro-structured surfaces including the machining parameters calculation and

Table 1 Tool parameters

	Calculate value	Actual value
Nose radius	1.58 mm	0.2 mm
Rake angle	–	0°
Clearance angle	3.9°	10°
Included angle	13.83°	60°

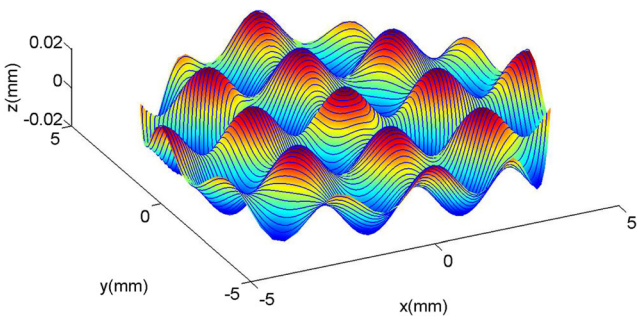

Fig. 15 Initial toolpath of the sinusoidal grid surface for calculating cutting parameters

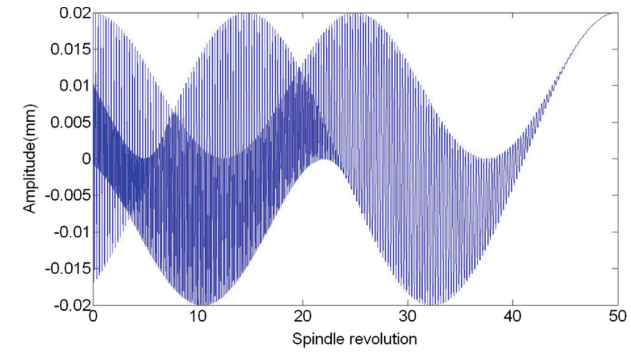

(a) FTS motion trajectory of initial tool path

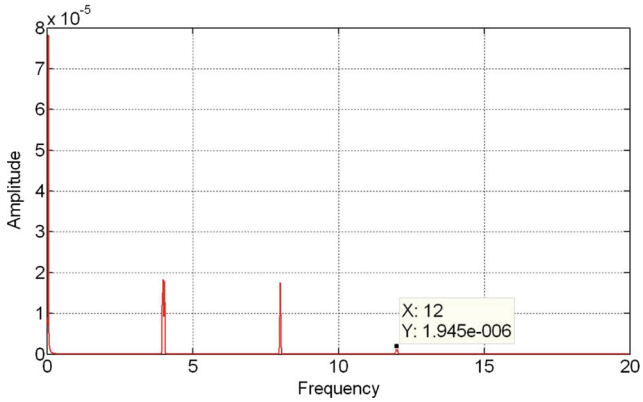

(b) Frequency spectrum of FTS motion trajectory

Fig. 16 Toolpath for calculation of spindle speed. **a** FTS motion trajectory of initial tool path. **b** Frequency spectrum of FTS motion trajectory

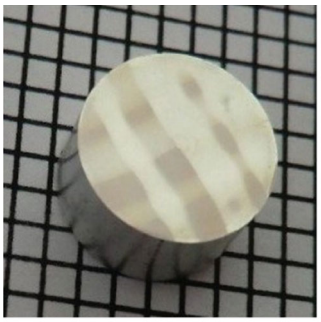

(a) The photo of the sinusoidal grid surface

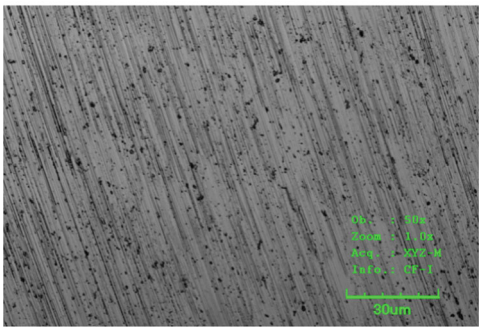

(b) The micro-topographies of the machined surface

Fig. 18 The photo of machined sinusoidal grid surface (**a**). **b** The micro-topographies of the machined surface

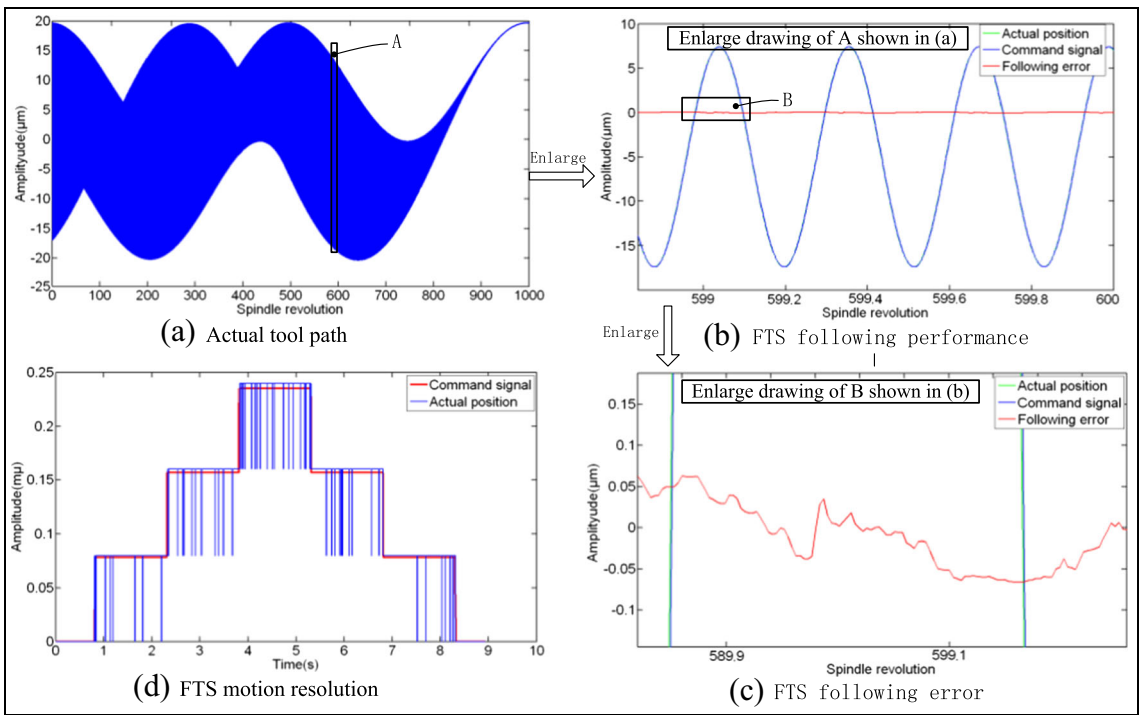

(a) Actual tool path

(b) FTS following performance

(c) FTS following error

(d) FTS motion resolution

Fig. 17 The actual toolpath and FTS working performance. **a** Actual tool path. **b** FTS following performance. **c** FTS following error. **d** FTS motion resolution

provide a new toolpath. Other researchers can fabricate the micro-structured surfaces referring to this paper.

Acknowledgments This work was jointly supported by the National Science Foundation of China (51175221) and the Department of Science and Technology of Jilin Province (20130522155JH).

References

1. Grossmann T, Wienhold T, Bog U, Beck T, Friedmann C, Kalt H, Mappes T (2013) Polymeric photonic molecule super-mode lasers on silicon. Light Sci Appl. doi:10.1038/lsa.2013.38
2. Gao W, Dejima S, Shimizu Y, Kiyono S (2003) Precision measurement of two-axis positions and tilt motions using a surface encoder. CIRP Ann 52:435–438
3. Kosten ED, Atwater JH, Parsons J, Polman A, Atwater HA (2013) Highly efficient GaAs solar cells by limiting light emission angle. Light Sci Appl. doi:10.1038/lsa.2013.1
4. Xiong W, Zhou YS, He XN, Gao Y, Mahjouri-Samani M, Jiang L, Baldacchini T, Lu YF (2012) Simultaneous additive and subtractive three-dimensional nanofabrication using integrated two-photon polymerization and multiphoton ablation. Light Sci Appl. doi:10.1038/lsa.2012.6
5. Zhang XD, Fang FZ, Wang HB, Wei GS, Hu XT (2009) Ultra-precision machining of sinusoidal surfaces using the cylindrical coordinate method. J Micromech Microeng 19:1–7
6. Zhu ZW, Zhou XQ, Liu ZW, Wang RQ, Zhu L (2014) Development of a piezoelectrically actuated two-degree-of-freedom fast tool servo with decoupled motions for micro-/nanomachining. Precis Eng 38(4):809–820
7. Yang ZJ, Zhou WB, Chen X, Chen XD, Li KT (2013) Modeling and optimal design of membrane based fast-tool-servo for freeform manufacturing of micro optical lens array. Adv Opt Manuf 552:411–414
8. Lu H, Lee D, Kim J, Kim S (2014) Modeling and machining evaluation of microstructure fabrication by fast tool servo-based diamond machining. Precis Eng 38(1):212–216
9. Lu H, Choi SC, Lee SM, Lee DW (2012) Microstructure of fast tool servo machining on copper alloy. Trans Nonferrous Metals Soc 22:820–824
10. Liu Q, Zhou XQ, Xu PZ, Zou Q (2012) A flexure-based long stroke fast tool servo for diamond turning. Int J Adv Manuf Technol 59(9–12):859–867
11. Yu DP, Gan SW, Wong YS, Hong GS, Rahman M, Yao J (2012) Optimized tool path generation for fast tool servo diamond turning of micro-structured surfaces. Int J Adv Manuf Technol 63(9–12):1137–1152
12. Yu DP, Wong YS, Hong GS (2011) A novel method for determination of the subsurface damage depth in diamond turning of brittle materials. Int J Mach Tools Manuf 51:918–927
13. Gao W, Araki T, Kiyono S, Okazaki Y, Yamanaka M (2003) Precision nano-fabrication and evaluation of a large area sinusoidal grid surface for a surface encoder. Precis Eng 27:289–298
14. Yu DP, Wong YS, Hong GS (2011) Optimal selection of machining parameters for fast tool servo diamond turning. Int J Adv Manuf Technol 57:85–99
15. Zhou M, Zhang HJ, Chen SJ (2010) Study on diamond cutting of nonrationally symmetric microstructured surfaces with fast tool servo. Mater Manuf Process 25:488–494
16. Suresh K, Yangd CH (1994) Constant scallop-height machining of free-form surfaces. ASME J Eng Ind 116:253–259